J. Fluid Mech. (1987), *vol.* 183, *pp.* 543–565
Printed in Great Britain

Resonant surface waves and chaotic phenomena

By X. M. GU AND P. R. SETHNA
Department of Aerospace Engineering and Mechanics, University of Minnesota, Minneapolis, MN 55455, USA

(Received 6 October 1986 and in revised form 25 March 1987)

Surface waves in a rectangular container subjected to vertical oscillations are studied. Effects of energy dissipation along the lines of Miles (1967) and the effect of surface tension are included. Sufficient conditions, for two modes to dominate the motion, are given. The analysis is along the lines of Miles (1984*a*) and Holmes (1986). A complete bifurcation analysis is performed, and the modal amplitudes and phases are shown to have chaotic behaviour. This result is obtained under assumptions different from those of Holmes (1986). The conclusions regarding chaotic motions are based on a theorem of Šilnikov (1970).

1. Introduction

The study of surface waves in vertically oscillating basins goes back to Faraday (1831). More recent studies start with Benjamin & Ursell (1954), who studied the linearized problem. Study of nonlinear phenomena falls into two categories. In one, it is assumed that only one spatial mode is dominant. This occurs under certain hypotheses. For a statement of these hypotheses and for references in this general area see Gu, Sethna & Narain (1987). In the other category, it is assumed that more than one spatial modes have motions of significant amplitude. For the main contributions, we refer to work by Miles (1976, 1984*a*, *b*, *c*, 1985) and Holmes (1986). For experimental work see Ciliberto & Gollub (1984, 1985), and for work in the presence of symmetry see Meron & Procaccia (1986). Much of this work is associated with the possibility of chaotic motions.

The work presented here is close to that of Miles (1984*a*) and to some extent to that of Holmes (1986). Both in Miles (1984*a*) and Holmes (1986), wave motions with two dominant spatial modes with frequencies that are in internal resonance are studied. In Miles (1984*a*) the frequency ratio is assumed to be equal to two, while in Holmes (1986) a detuning parameter is introduced so that the ratio can be a number in a small neighbourhood of two. In both studies the container is assumed to be excited sinusoidally in the vertical direction. Both studies are based on a Hamiltonian formulation. In Miles (1984*a*) the problem is studied under the assumption that the nonlinear effects, the parametric excitation, and the effects of dissipation are all small and of the same order of magnitude. In Holmes (1986) it is assumed that the excitation effects and dissipation are higher-order quantities when compared with the nonlinear effects.

Our work follows fairly closely the work of Miles (1984*a*). We, however, study in detail the coupling effects of the spatial modes and give conditions under which internal resonances of the type discussed here can occur. Furthermore, we take into account the detuning in the internal resonances, which make it possible for the system to have Hopf bifurcations. Moreover, the occurrence of the Hopf bifurcations

introduces a subset in the parameter space in which no stable periodic or quasi-periodic motions occur. We show that chaotic phenomena occur in this interval. Our results are based on a theorem of Šilnikov and are verified by numerical computations. We thus show that chaotic behaviour is possible, in contrast to the work of Holmes (1986), when the system is not perturbed from a completely integrable Hamiltonian system; furthermore, we show that the amplitudes and phases of the dominant modes can have quite general chaotic behaviour as a function of time as compared with the special type of chaotic behaviour of motions described in Holmes (1986).

We conjecture that a more elaborate analysis involving more modes and done at a higher approximation may exhibit surface-wave phenomena of very complicated nature. Miles (1985), on the other hand shows that, at least in the case of wave motions excited by horizontal motions of the basin, chaotic behaviour occurs only with a two-mode approximation and, based on some numerical work, he shows that no chaotic behaviour is possible at higher-mode approximation. He remarks, however, that the chaotic behaviours may be an artifact of the truncation and that 'the anomalous effects of truncation ... appear to be associated with the confluence of internal resonances in the limiting of vanishing dispersion'. We feel the introduction of parameters that disrupt exact tuning would remove this confluence, and this may validate our conjecture.

We also give a discussion of the difficulties associated with an experimental study of the type of wave motion studied here.

2. Problem formulation

Following closely the discussion by Gu (1986), consider a rigid rectangular container containing an inviscid incompressible fluid. The container is subjected to vertical motions $f(t) = -\Delta \cos \omega t$ with respect to a fixed reference frame. We assume that the flow is irrotational and, thus, there exists a potential function $\phi(\boldsymbol{x}, t)$, where $\boldsymbol{x}$ is the position with respect to the container, so that $\nabla\phi = \boldsymbol{V}$, where $\boldsymbol{V}$ is the fluid velocity relative to the container, and, due to the incompressibility, ϕ satisfies Laplace's equation. The origin of a moving Cartesian reference frame is attached to the container at the undisturbed free surface of the fluid. The cross-section of the container is assumed to be rectangular of sides a and b and the fluid depth is h. The gravitational acceleration and the surface tension are denoted by g and $\overline{\gamma}$ respectively. The free surface is denoted by $z = \eta(x, y, t)$.

Let

$$\Delta = \epsilon b \Delta', \quad x = bx', \quad y = by', \quad z = bz', \quad t = \frac{1}{\omega} t',$$

$$\phi = \epsilon \omega b^2 \phi', \quad \eta = \epsilon b \eta', \quad G = \frac{g}{\omega^2 b}, \quad \gamma = \frac{\overline{\gamma}}{\rho \omega^2 b^3}, \quad a' = \frac{a}{b}, \quad h' = \frac{h}{b},$$

where ϵ is a small parameter. Dropping the primes for simplicity, we obtain the field equations and boundary conditions in dimensionless form as follows. The potential function satisfies:

$$\nabla^2 \phi = 0, \quad \text{in } 0 \leqslant x \leqslant a, \quad 0 \leqslant y \leqslant 1, \quad -h \leqslant z \leqslant \epsilon \eta(x, y, t), \tag{2.1}$$

along with the boundary conditions on the rigid walls:

$$\left.\begin{aligned} \phi_x &= 0 \quad \text{on } x = 0, a, \\ \phi_y &= 0 \quad \text{on } y = 0, 1, \\ \phi_z &= 0 \quad \text{on } z = -h. \end{aligned}\right\} \tag{2.2}$$

The boundary conditions on the free surface, $z = \epsilon\eta(x, y, t)$, take the form

$$\phi_t + \tfrac{1}{2}\epsilon(\nabla\phi)^2 + (G + \epsilon\Delta\cos t)\,\eta = \gamma[(\eta_{xx}+\eta_{yy}) - \tfrac{1}{2}\epsilon^2(\eta_{xx}\eta_y^2 + \eta_{yy}\eta_x^2 + 3\eta_{xx}\eta_x^2 + 3\eta_{yy}\eta_y^2 + 4\eta_x\eta_y\eta_{xy})] + O(\epsilon^3), \quad (2.3)$$

$$\phi_z = \epsilon[\phi_x\eta_x + \phi_y\eta_y] + \eta_t, \quad (2.4)$$

and from the incompressibility of the fluid, we have the condition

$$\int_0^1\int_0^a \eta(x, y, t)\,\mathrm{d}x\,\mathrm{d}y = 0. \quad (2.5)$$

3. Asymptotic analysis

We assume the nth-order asymptotic expansion of the solution of (2.1)–(2.5), asymptotic as $\epsilon \to 0$, of the form

$$\left.\begin{aligned} \phi &= \phi(x, y, z, \boldsymbol{a}, \boldsymbol{\theta}, t, \epsilon) = \sum_{n=0}^{N}\sum_{ij=0}^{\infty} \epsilon^n q_{ij}^{(n)}(t)\,S_{ij}(x, y)\,g_{ij}(Z), \\ \eta &= \eta(x, y, \boldsymbol{a}, \boldsymbol{\theta}, t, \epsilon) = \sum_{n=0}^{N}\sum_{ij=0}^{\infty} \epsilon^n p_{ij}^{(n)}(t)\,S_{ij}(x, y), \end{aligned}\right\} \quad (3.1)$$

where $$S_{ij}(x, y) = \cos\frac{i\pi x}{a}\cos j\pi y, \quad g_{ij}(z) = \cosh K_{ij}(h+z)\cosh^{-1} K_{ij}h, \quad (3.2)$$

$$K_{ij}^2 = \pi^2\left[\frac{i^2}{a^2} + j^2\right].$$

When $\epsilon = 0$ we have

$$p_{ij}^{(0)}(t) = a_{ij}\cos(\mu_{ij}t + \theta_{ij}), \quad q_{ij}^{(0)}(t) = -\frac{\mu_{ij}}{\alpha_{ij}}a_{ij}\sin(\mu_{ij}t + \theta_{ij}), \quad (3.3)$$

where $$\mu_{ij} = [(G + \gamma K_{ij}^2)\,\alpha_{ij}]^{\frac{1}{2}}, \quad \alpha_{ij} = k_{ij}\tanh k_{ij}a,$$

and a_{ij} and θ_{ij} are arbitrary constants. For $i = j = 0$, (2.5) yields $p_{00}^{(0)} = 0$ and $q_{00}^{(0)} = 0$.

When $\epsilon \neq 0$, the method of analysis used is an adaptation of the method of averaging as given by Mitropolsky (1965) and as employed by Bajaj & Sethna (1980). The solution is assumed to depend on two infinite-dimensional vectors $\boldsymbol{a}$ and $\boldsymbol{\theta}$, the time derivative of which will be quantities of $O(\epsilon)$ as follows:

$$\dot{a}_{ij} = \sum_{n=1}^{N} \epsilon^n A_{ij}^{(n)}(\boldsymbol{a}, \boldsymbol{\theta}) \quad (i, j = 0, 1, 2, \ldots, \quad i = j \neq 0), \quad (3.4)$$

$$\dot{\theta}_{ij} = \sum_{n=1}^{N} \epsilon^n B_{ij}^{(n)}(\boldsymbol{a}, \boldsymbol{\theta}) \quad (i, j = 0, 1, 2, \ldots, \quad i = j \neq 0). \quad (3.5)$$

Substituting (3.1) into (2.3) and (2.4), taking into account (3.4) and (3.5), equating equal powers of ϵ, and taking projections, we have (for details see Gu 1986)

$$\frac{\mathrm{d}p_{mn}^{(1)}}{\mathrm{d}t} - \alpha_{mn}q_{mn}^{(1)} = -\left[\frac{\partial p_{mn}^{(0)}}{\partial a_{mn}}A_{mn}^{(1)} + \frac{\partial p_{mn}^{(0)}}{\partial \theta_{mn}}B_{mn}^{(1)}\right] - G_{ijrs}^{(1)\,mn}\,p_{ij}^{(0)}\,q_{rs}^{(0)}, \quad (3.6)$$

$$\frac{\mathrm{d}q_{mn}^{(1)}}{\mathrm{d}t} + \frac{\mu_{mn}^2}{\alpha_{mn}}p_{mn}^{(1)} = -\Delta\cos p_{mn}^{(0)} - \left[\frac{\partial q_{mn}^{(0)}}{\partial a_{mn}}A_{mn}^{(1)} + \frac{\partial q_{mn}^{(0)}}{\partial \theta_{mn}}B_{mn}^{(1)}\right] - \left[\tfrac{1}{2}G_{ijrs}^{(2)\,mn}\,q_{ij}^{(0)}\,q_{rs}^{(0)} + G_{ijrs}^{(3)\,mn}\,p_{ij}^{(0)}\frac{\partial q_{rs}^{(0)}}{\partial t}\right], \quad (3.7)$$

for terms of order ϵ. In (3.6) and (3.7) the repeated subscripts, except m and n, imply summation from zero to infinity. The quantities $G^{(n)}_{ijrs}{}^{mn}$ are complicated expressions, as given in the Appendix, and are not zero when the equations of the involved modes are spatially coupled with the (m,n)th mode.

3.1. *Coupling phenomena*

The system of equations (3.6), (3.7) and those of higher order can be studied under a variety of assumptions on the physical parameters. Qualitatively different phenomena occur depending on the coupling between the infinity of equations at each approximation.

An examination of coefficients $G^{(u)}_{ijrs}{}^{mn}$ for $u = 1, 2, 3$, which determine spatial dependence, shows (see Appendix) that for modes with mode numbers (i,j) and (r,s) to couple at $O(\epsilon)$, and therefore to affect the mode with mode numbers (m,n), the following conditions have to be satisfied:

$$i \pm r \pm m = 0, \quad j \pm s \pm n = 0, \tag{3.8}$$

where i, j, r, s, n and m are all non-negative integers. In general, therefore, all modes are coupled with all other modes, but not directly, and in a pattern dictated by (3.8).

In the main body of this study we discuss the case when only two spatial modes, in the scaled variables of (2.1)–(2.4), have motions of amplitude $O(\epsilon^0)$ and all other modes have motions of amplitude at least of order ϵ. Later we discuss the possibility of more complicated cases.

Suppose the (m,n)th mode is in external subharmonic resonance ($\mu_{mn} \approx \frac{1}{2}$), then within the restriction of a two-mode analysis we observe that either (i,j) or (r,s) must be equal to (m,n) and the other mode must have one of the three mode numbers: $(2m, 2n)$, $(0, 2n)$ and $(2m, 0)$; in the case where neither m nor n is zero, the other mode may also have mode number $(\frac{1}{2}m, \frac{1}{2}n)$, if both m and n are even. If $m = 0$ and $n \neq 0$, the other mode must have mode numbers $(0, 2n)$ or $(p, \frac{1}{2}n)$ for any positive integer p, and similarly for the case when $m \neq 0$ and $n = 0$.

In the subsequent analysis we introduce energy dissipation in a manner similar to that by Miles (1984*a*) and Holmes (1986). Due to the presence of this dissipation, in order that a mode has sustained oscillation, it must not only satisfy the requirements of model coupling according to condition (3.8), but it must also satisfy certain conditions on its natural frequency so as to be able to get energy through resonance phenomena. There are two distinct cases: the superharmonic case when the coupled mode has a frequency almost twice that of the (m,n)th mode, and the subharmonic case when the coupled mode has a frequency near half that of the (m,n)th mode. If neither m nor n is zero, then the former case is possible, only if the coupled mode has one of the mode numbers $(2m, 2n)$, $(0, 2n)$ and $(2m, 0)$; and the latter case is possible when m and n are even, and when the coupled mode has mode number $(\frac{1}{2}m, \frac{1}{2}n)$ and a frequency about half that of the (m,n)th mode. On the other hand, if say $m = 0$, then the former case is also possible even when the other mode has mode number $(p, \frac{1}{2}n)$ for sufficiently large p.

4. The basic finite dimensional equations

Limiting the discussion to the superharmonic case let

$$\mu^2_{mn} = (\tfrac{1}{2})^2 + \epsilon\sigma_1, \tag{4.1}$$

$$\frac{\mu^2_{ij}}{\mu^2_{mn}} = 4 + \epsilon\sigma_{ij}. \tag{4.2}$$

where σ_i is the external, and σ_{ij} the internal detuning parameters, respectively. The integers (i,j) in (4.1) and (4.2) take values $(2m,2n)$, $(2m,0)$ or $(0,2n)$.

Inserting (4.1) and (4.2) in (3.6) and (3.7), and imposing the condition that the latter has periodic solutions when a_{ij} and θ_{ij} are regarded as constants, we solve for $A^{(1)}_{mn}$ and $B^{(1)}_{mn}$, using the 'Fredholm Alternative' (Hale 1969). Substituting for the functions $A^{(1)}_{mn}$ and $B^{(1)}_{mn}$ and in (3.4) and (3.5) we have

$$\left.\begin{aligned}
\dot{a}_{mn} &= \epsilon[-d_{mn}a_{mn}+\Delta_{mn}a_{mn}\sin 2\theta_{mn}+\Gamma_{mn}a_{ij}a_{mn}\sin(2\theta_{mn}-\theta_{ij}),\\
a_{mn}\dot{\theta}_{mn} &= \epsilon[\sigma_1+\Delta_{mn}\cos 2\theta_{mn}+\Gamma_{mn}a_{ij}\cos(2\theta_{mn}-\theta_{ij})]a_{mn},\\
\dot{a}_{ij} &= \epsilon[-\nu_d d_{mn}a_{ij}-\Gamma_{ij}a^2_{mn}\sin(2\theta_{mn}-\theta_{ij})],\\
a_{ij}\dot{\theta}_{ij} &= \epsilon[(2\sigma_1+\tfrac{1}{8}\sigma_{ij})a_{ij}+\Gamma_{ij}a^2_{mn}\cos(2\theta_{mn}-\theta_{ij})].
\end{aligned}\right\} \tag{4.3}$$

where

$$\Gamma_{mn} = G^{(1)\,mn}_{ijmn}\frac{1}{8\alpha_{mn}}-G^{(1)\,mn}_{mnij}\frac{1}{4\alpha_{ij}}+G^{(2)\,mn}_{mnij}\frac{1}{4\alpha_{ij}}-G^{(3)\,mn}_{ijmn}\tfrac{1}{8}-G^{(3)\,mn}_{mnij}\frac{\alpha_{mn}}{2\alpha_{ij}},\quad \Delta_{mn}=\tfrac{1}{2}\Delta\alpha_{mn}, \tag{4.4}$$

$$\Gamma_{ij} = -G^{(1)\,ij}_{mnmn}\frac{1}{8\alpha_{mn}}-\alpha_{ij}\left[G^{(2)\,ij}_{mnmn}\frac{1}{32\alpha^2_{mn}}+G^{(3)\,ij}_{mnmn}\frac{1}{16\alpha_{mn}}\right], \tag{4.5}$$

where, for given (m,n), (i,j) may be one of the pairs of integers mentioned above.

In (4.3) we have introduced damping as in Miles (1984*a*) as first-order terms. The amplitudes of all the modes other than the two modes under consideration satisfy equations of the form

$$\dot{a}_{uv} = -d_{uv}a_{uv},$$

and thus $a_{uv}(t)\to 0$ as $t\to\infty$.

$$\left.\begin{aligned}
\text{Let}\qquad t' &= \frac{1}{\epsilon\Delta_{mn}}t'',\quad a_{mn}=\Delta_{mn}(\Gamma_{mn}\Gamma_{ij})^{-\frac{1}{2}}a_1,\quad a_{ij}=\Delta_{mn}\Gamma^{-1}_{mn}a_2,\\
d_{mn} &= \Delta_{mn}d,\quad \sigma_1=\Delta_{mn}\sigma,\quad \sigma_{ij}=8\beta,\\
\theta_{mn} &= \theta_1,\quad \theta_{ij}=\theta_2,
\end{aligned}\right\} \tag{4.6}$$

and using an overdot to denote the derivative with respect to t, we obtain

$$\left.\begin{aligned}
\dot{a}_1 &= -da_1+a_1\sin 2\theta_1+a_1a_2\sin(2\theta_1-\theta_2),\\
a_1\dot{\theta}_1 &= [\sigma+\cos 2\theta_1+a_2\cos(2\theta_1-\theta_2)]a_1,\\
\dot{a}_2 &= -\nu_d da_2-a^2_1\sin(2\theta_1-\theta_2),\\
a_2\dot{\theta}_2 &= (2\sigma+\beta)a_2+a^2_1\cos(2\theta_1-\theta_2).
\end{aligned}\right\} \tag{4.7}$$

In Cartesian coordinates

$$x_1 = a_1\cos\theta_1, y_1 = -a_1\sin\theta_1,$$
$$x_2 = a_2\cos\theta_2, y_2 = -a_2\sin\theta_2,$$

we have

$$\left.\begin{aligned}
\dot{x}_1 &= -\mathrm{d}x_1-(1-\sigma)y_1-y_1x_2+x_1y_2,\\
\dot{y}_1 &= -\mathrm{d}y_1-(1+\sigma)x_1-x_1x_2-y_1y_2,\\
\dot{x}_2 &= -\nu_d\,\mathrm{d}x_2+(2\sigma+\beta)y_2+2x_1y_1,\\
\dot{y}_2 &= -\nu_d\,\mathrm{d}y_2-(2\sigma+\beta)x_2-x^2_1+y^2_1.
\end{aligned}\right\} \tag{4.8}$$

Furthermore if $\bar{x}_1 = (2x)^{\frac{1}{2}}, \bar{y}_1 = -(2y_1)^{\frac{1}{2}}, \bar{x}_2 = x_2, \bar{y}_2 = -y_2$, then (4.8) can be written in Hamiltonian form. If the damping terms are dropped, and $\beta = 0$, equations (4.8) are equivalent to that of Miles (1984*a*).

Equations (4.8) are in the general category of equations studied by Lorenz (1984). Although (4.8) have only a superficial similarity in structure to the now famous equations of Lorenz (1963), we will show later that they have a strong similarity in the behaviour of the solutions.

5. Periodic and quasi-periodic solutions and their bifurcations

If a_i and θ_i $(i = 1, 2)$, are constants, then we have periodic solutions of the original system. The amplitudes of the periodic motions are:

$$\left.\begin{aligned} a_1^2 &= \sigma(2\sigma+\beta) - \nu_d d^2 \pm \{R - [d(2\sigma+\beta) + \nu_d d\sigma]^2\}^{\frac{1}{2}}, \\ a_2^2 &= \frac{a_1^4}{R}. \end{aligned}\right\} \tag{5.1}$$

The 'response curves', plots of a_1 versus σ, are given in figure 1, with $\beta = -1.0$ and several values of d.

If $R = \nu_d^2 d^2 + (2\sigma+\beta)^2$ and $k = a_2^2/a_1^2$, then the phase angles can be shown to take two values, with a phase difference of π, for each solution in (5.1) as follows:
if $-\sigma + (2\sigma+\beta)k^2 > 0$,

$$\theta_1 = \begin{cases} \frac{1}{2}\arctan\dfrac{d(1+\nu_d k^2)}{-\sigma+(2\sigma+\beta)k^2}, \\ \pi + \frac{1}{2}\arctan\dfrac{d(1+\nu_d k^2)}{-\sigma+(2\sigma+\beta)k^2}; \end{cases}$$

if $-\sigma + (2\sigma+\beta)k^2 < 0$,

$$\theta_1 = \begin{cases} \frac{1}{2}\pi - \frac{1}{2}\arctan\dfrac{d(1+\nu_d k^2)}{-\sigma+(2\sigma+\beta)k^2}, \\ \frac{3}{2}\pi - \frac{1}{2}\arctan\dfrac{d(1+\nu_d k^2)}{-\sigma+(2\sigma+\beta)k^2}; \end{cases} \tag{5.2}$$

if $2\sigma+\beta < 0$,

$$\theta_2 = 2\theta_1 - \arctan\frac{\nu_d d}{2\sigma+\beta};$$

if $2\sigma+\beta > 0$,

$$\theta_2 = -\pi + 2\theta_1 - \arctan\frac{\nu_d d}{2\sigma+\beta}.$$

An examination of (5.1) shows that if

$$s_1 = d^2 + \sigma^2 - 1 \quad (d > 0), \tag{5.3}$$

$$s_2 = \nu_d^2 d^2 + (2\sigma+\beta)^2 - [d(2\sigma+\beta) + \nu_d d\sigma]^2, \tag{5.4}$$

$$s_3 = \nu_d d^2 - \sigma(2\sigma+\beta), \tag{5.5}$$

then the surfaces $s_1 = 0$, $s_2 = 0$ and $s_3 = 0$ divide the (σ, d, β) parameter space into several open subsets, so that for parameter values in each of these sets, a different number of constant solutions occur.

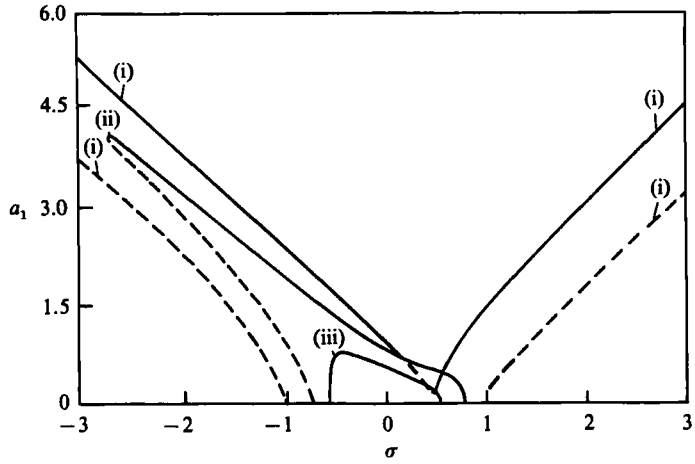

FIGURE 1. Response curves (a_1 *vs.* σ) for $\beta = -1.0$ and different dampings: (i) $d = 0.1$; (ii) $d = 0.6325$; (iii) $d = 0.8367$. ——, stable branch; – – – –, unstable branch.

For a fixed β, we study a slice of the bifurcation diagram in the (σ, d)-plane. The curve $s_1 = 0$ for $d > 0$ is a semicircle. Now $s_3 = 0$ for a fixed β is a hyperbola with its centre at $(-\frac{1}{4}\beta, 0)$, apexes at $(0,0)$ and $(-\frac{1}{2}\beta, 0)$ and the asymptotes $d = \pm(2/\nu_d)^{\frac{1}{2}}(\sigma + \frac{1}{4}\beta)$. For $\beta = 0$, the hyperbola degenerates to two intersecting straight lines $d = \pm(2/\nu_d)^{\frac{1}{2}}\sigma$. When $|\beta| \leqslant 2$, the two branches of the hyperbola intersect the semicircle at A and B coordinates $(\sigma_A, (1-\sigma_A^2)^{\frac{1}{2}})$ and $(\sigma_B, (1-\sigma_B^2)^{\frac{1}{2}})$, where

$$\sigma_{A,B} = \frac{-\beta \pm (\beta^2 + 8\nu_d + 4\nu_d^2)^{\frac{1}{2}}}{2(2+\nu_d)}.$$

When $|\beta| > 2$, the apex $(-\frac{1}{2}\beta, 0)$ is outside the semicircle, hence only one branch of the hyperbole intersects it.

Furthermore, it can then be shown that $s_2 = 0$ is tangent to the semicircle at A and B and that

$$\lim_{\sigma \to \infty} d = \frac{2}{2+\nu_d}, \quad \lim_{d \to \infty} \sigma = \frac{\pm\nu_d - \beta}{2+\nu_d}.$$

The eigenvalues of the zero solution of (4.8) are:

$$\lambda_{1,2} = -d \pm (1-\sigma^2)^{\frac{1}{2}}, \quad \lambda_{3,4} = -\nu_d d \pm (2\sigma + \beta)\mathrm{i}. \tag{5.6}$$

Since $d > 0$, the solution cannot have pure imaginary eigenvalues and thus it cannot go through a Hopf bifurcation. The solution is stable if $\sigma > (1-d^2)^{\frac{1}{2}}$ or $\sigma < -(1-d^2)^{\frac{1}{2}}$, and unstable if $-(1-d^2)^{\frac{1}{2}} < \sigma < (1-d^2)^{\frac{1}{2}}$. If $\sigma = \pm(1-d^2)^{\frac{1}{2}}$, a zero eigenvalue occurs, and an elementary analysis shows that the bifurcations are pitchfork bifurcations on $s_1 = 0$, which can be either super- or subcritical.

If the characteristic equation of the linearized system near a constant solution is the following quartic equation

$$J_4\lambda^4 + J_3\lambda^3 + J_2\lambda^2 + J_1\lambda + J_0 = 0, \tag{5.7}$$

then, using the Routh–Hurwitz conditions (Routh 1877), the necessary and sufficient conditions for the constant solutions to be stable are

$$\text{(i)}\ J_0 > 0,$$
$$\text{(ii)}\ J_1 > 0,$$
$$\text{(iii)}\ J_3 J_4 > 0,$$
and $$\text{(iv)}\ J_1(J_2 J_3 - J_1 J_4) - J_0 J_3^2 > 0; \tag{5.8}$$

where
$$J_4 = 1,$$
$$J_3 = 2(1+\nu_d)\,d,$$
$$J_2 = R(1+4k^2) + 4\nu_d\, d^2,$$
$$J_1 = 2Rd[1+2(1+\nu_d)\,k^2],$$
$$J_0 = -4Rk^2[\sigma(2\sigma+\beta) - \nu_d\, d^2 - Rk^2]. \tag{5.9}$$

Conditions (ii) and (iii) are obviously satisfied for any physical system. Substituting from (5.1) in (5.9) we can show that

$$J_0 = \pm 4Rk^2\{R - [d(2\sigma+\beta) + \nu_d\, d\sigma]^2\}^{\frac{1}{2}}, \tag{5.10}$$

where the plus and minus signs are for the upper and the lower branches of the response curves (figure 1), respectively. The upper branch is thus stable if (iv) is also satisfied, but the lower branch is always unstable.

Let

$$s_4\left(\sigma, d, \beta, \frac{a_1^2}{R}\right) = 2(1+\nu_d^2)\frac{a_1^2}{R}[(\nu_d^2+2\nu_d)\,d^2 + (2\sigma+\beta)\,(4\sigma+\beta)] + \nu_d[(2\sigma+\beta)^2 + \nu_d^2\, d^2 + 4d(1+\nu_d)]. \tag{5.11}$$

Then (iv) is equivalent to $s_4 > 0$. If $\beta/\sigma > -2$ or $\beta/\nu < -4$, it is clear that $s_4 > 0$ and (iv) is satisfied, and the upper branch is stable. On the other hand, $-4 < \beta/\sigma < -2$ is a necessary condition for instability of the upper branch by Hopf bifurcation.

The condition for at least one pair of pure imaginary eigenvalues to occur is $s_4 = 0$. Thus to have a Hopf bifurcation, $s_4 = 0$ and, furthermore, the eigenvalues must traverse the pure imaginary axis transversally. Substituting for a_1^2 with a plus sign from (5.1) in s_4 we have

$$\tilde{H}(\sigma, d, \beta) = s_4\left(\sigma, d, \beta, \frac{a_1^2(\sigma, d, \beta)}{R(\sigma, d, \beta)}\right). \tag{5.12}$$

Then a condition for Hopf bifurcation is that

$$\tilde{H}(\sigma, d, \beta) = 0. \tag{5.13}$$

Numerical computation shows that Hopf bifurcations are possible for $0 < |\beta| < 2.67$ and $d < 0.243$. For given values of β and d satisfying these inequalities, the condition (5.13) gives two values of σ, $\sigma = \sigma_{\mathrm{H1}}$ and σ_{H2} with $\sigma_{\mathrm{H1}} < \sigma_{\mathrm{H2}}$, and for σ near σ_{H1} and σ_{H2}, periodic motions are possible. In figure 2, the zeros of (5.13) are plotted for several values of β, $0 < \beta < 2.67$. Those for $-2.67 < \beta < 0$ are symmetric with a reflection in the $\sigma = 0$ axis. They appear approximately as semicircles. We denote the interior of the semicircle as set IV.

For each given $|\beta| < 2.67$, there exists a limiting value of $d = d^*$. If $d > d^*$, then no Hopf bifurcation occurs. Values of d^* are plotted versus β in figure 2 as the envelope of set IV.

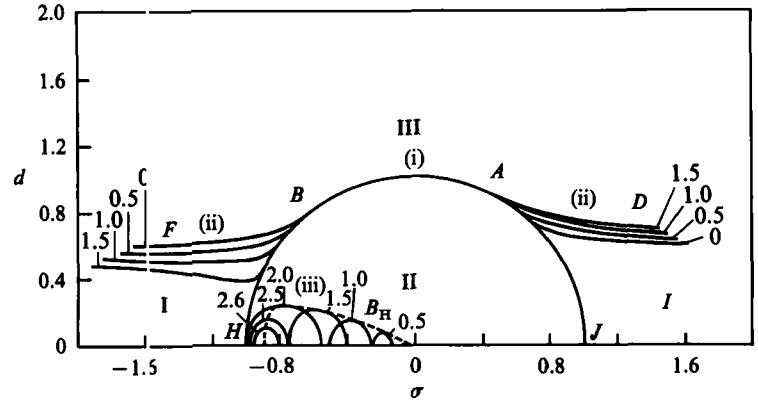

FIGURE 2. Bifurcation diagram on (σ, d)-plane for different β (as indicated). (i) Pitchfork; (ii) Saddle-node; (iii) Hopf. The diagram is a reflection in the axis $\sigma = 0$ for negative β.

We remark that if β is zero, (iv) always holds for all given d and σ; thus Hopf bifurcations are impossible. Since β represents detuning in internal resonance, this means that the linear natural frequencies of the interacting modes must deviate from the ratio 2 in order that Hopf bifurcations occur. Miles (1984*a*) shows this non-occurrence of Hopf bifurcations.

We now can summarize the results as follows: In set I, there are three sinks and two saddles; in set III, only one sink; in set II, two sinks and a saddle; and in set IV three saddles.

On AJ and BH of the unit semicircle, a pitchfork bifurcation occurs. In this bifurcation, as the parameter pair (σ, d) crosses from region I to region II, a sink (the zero solution) loses its stability as two saddles and this sink coalesce into a saddle. Globally, the total of five equilibria including two saddles and three sinks, become two sinks and one saddle.

On AB of the unit semicircle, a pitchfork bifurcation of another type occurs. In contrast to the one stated above, as the parameter pair (σ, d) crosses from region III to region II, a sink (the zero solution) loses its stability and becomes a saddle and two sinks. A local analysis on the centre manifold shows that if $\sigma(2\sigma+\beta)-\nu_d d^2 > 0$, the pitchfork bifurcation is subcritical and if $\sigma(2\sigma+\beta)-\nu_d d^2 < 0$, the pitchfork bifurcation is supercritical. This justifies the above statement.

As the parameter pair (σ, d) crosses from region I into region III through the curve AD or BF, the origin remains a sink, and a saddle and a node, and another saddle and another node coalesce simultaneously in a double saddle-node bifurcation and the only fixed point left is the stable zero solution. All the above statements have been verified analytically.

At the exceptional bifurcation points A and B, at which AD and BF are tangent to the unit semicircle, the zero solution and non-zero fixed points simultaneously undergo degenerate pitchfork bifurcations with saddle-node and pitchfork bifurcations occurring simultaneously.

As we go from sets II to IV on the boundary of set IV, the two sinks (stable non-zero solutions) become non-hyperbolic with a pair of pure imaginary eigenvalues, and they have Hopf bifurcations simultaneously. Using centre manifold theory and averaging procedure in a manner similar to that in Sethna & Gu (1985), we are able to tell the stabilities of the limit cycles created from the Hopf bifurcations and their approxi-

mate radii. For $\beta = -1$ explicit calculations show that the bifurcation is super- and subcritical on the left-hand and right-hand boundaries of set IV, respectively.

The constant solutions in sets I, II and III represent periodic solutions. Which of the multiple stable solutions will occur depends on basins of attraction of these stable solutions in the four-dimensional state space. On the boundary of set IV, the motion becomes amplitude modulated at a very low frequency. The system has complicated behaviour for values of σ inside set IV, which behaviour we discuss in the next section. Here we merely note that the damping parameter d has to be small for these complicated phenomena to occur.

6. Global bifurcations – Šilnikov theorem – routes to chaos

In this section we study complex global bifurcations that lead to chaotic motions for values of parameters in set IV.

6.1. *General properties*

Consider the Cartesian form (4.8) of the system equations. They have the symmetry $(x_1, y_1, x_2, y_2) \to (-x_1, -y_1, x_2, y_2)$. Hence the fixed points, trajectories, limit cycles, attractors, etc., occur in pairs if they are not taken into themselves by the symmetry.

Following the method of Lorenz (1963), for the three-dimensional equations, it can be shown (Gu 1986) that there exists a hyper-ellipsoid S in R^4 on which the vector field is directed everywhere inwards. If the interior of S is D, then all trajectories entering D remain in D for all $t > 0$, and thus D must contain at least one attracting set. Furthermore, from an examination of (4.8), it is seen that the divergence of the flow is equal to $-2(1+\nu_d)\,d$, which is always negative. The flow is thus contracting and the above mentioned attracting set must have zero four-dimensional volume.

We also note from (4.8) that the two-dimensional subset $x_1 = y_1 = 0$ is an invariant set. Furthermore, the flow on this subset is globally spiralling into the origin. This is because $x_1 = y_1 = 0$ means no motion of the mode excited by external resonance and thus the motion in the other internally resonant mode represented by (x_2, y_2) decays to zero.

Our result depends in part on a theorem of Šilnikov (1970). The hypotheses of the theorem are that the system has a homoclinic orbit (i.e. an orbit that approaches the fixed point as $t \to +\infty$ and as $t \to -\infty$) at a fixed point and the fixed point has one pair of complex conjugate eigenvalues with negative real parts, one negative eigenvalue and one positive eigenvalue. Furthermore, the absolute value of the real part of the complex eigenvalues are assumed to be smaller than the magnitude of the real eigenvalues. Under these assumptions, the system is shown to have a countable number of three-dimensional Smale horseshoes, and thus the dynamics on the horseshoe is homeomorphic to the Bernoulli shift of n symbols (Lichtenberg & Lieberman 1982). The occurrence of the horseshoes is accompanied by and generates certain types of behaviour in the solutions of system (4.8).

We have a flow with contracting volume, and for such flows the creation of horseshoes is accompanied by sequences of bifurcations (Yorke & Alligood 1985; Gavrilov & Šilnikov 1972, 1973). We will show that in our problem there occurs at least one sequence of bifurcation, which includes a period-doubling sequence of periodic motions that is associated with the horseshoes generated by the Šilnikov phenomenon.

The horseshoes themselves can generate different phenomena. They can generate very long transients, which appear superficially as chaotic motions, before the orbit

asymptotes, as $t \to \infty$, to a stable fixed point, a stable periodic orbit or some other relatively simple stable invariant set. Such behaviour is called 'preturbulence' (Kaplan & Yorke 1979). The existence of the horseshoes can also generate a 'strange attractor' (Guckenheimer & Holmes 1983), which itself is an invariant set, and the solution appears to be chaotic for all time. Both preturbulence and strange-attractor behaviour occur in our problem.

In physical terms, in the case of preturbulence, the amplitudes and phases of the two spatial modes show chaotic behaviour for a considerable time before they settle to constant values, which represent steady periodic waves. In the case when a strange attractor is formed, the amplitudes and phases of the two spatial modes exhibit sustained chaotic behaviour.

The Šilnikov theorem proves the occurrence of horseshoes in an open interval in the parameter space containing the parameter values at homoclinicity. In our problem, due to some special features, numerical results showing chaotic behaviour appear to be in a half-open interval. The sources of this behaviour will be discussed later.

Numerical studies were done with a view to find the location of stable as well as unstable periodic orbits, and special methods were used to determine the Floquet multipliers of these orbits. For both periodic and chaotic orbits, power-spectrum computations using fast Fourier transforms were done and, where appropriate, three-dimensional Poincaré-mappings of the flow in R^4 were taken.

The numerical work is limited to a special case when $d = 0.1$, $\beta = -1.0$ and $\nu_d = d_2/d_1 = \sqrt{2}$. The parameters are chosen so that Hopf bifurcations are possible and so that we have a comparatively wide interval of external detuning parameter in which global bifurcations occur. Following Miles (1967), it is not difficult to show that the value $\sqrt{2}$ is a good approximation for the damping ratio in the case in which the (m, n)th mode is coupled with the $(2m, 2n)$th mode. Hopf bifurcations occur for the above value of d and β at $\sigma = \sigma_{H1} = 0.292479$ and $\sigma = \sigma_{H2} = 0.470699$. The former is supercritical and the latter subcritical.

All the phenomena described in this section occur in set IV. There are always three fixed points, since the condition $|\sigma| < (1-d^2)^{\frac{1}{2}}$ is satisfied. The origin, labelled O throughout, has its eigenvalues as in (5.6). There is one positive and one negative eigenvalue and a pair of complex conjugate eigenvalues with negative real parts.

The two non-zero fixed points, labelled as A and B throughout, always have two pairs of complex conjugate eigenvalues. They are stable when $\sigma < \sigma_{H1}$ and $\sigma > \sigma_{H2}$. They become unstable simultaneously through Hopf bifurcations when $\sigma = \sigma_{H1}$ and $\sigma = \sigma_{H2}$, with the real parts of one pair of eigenvalues crossing the pure imaginary axis. In figure 3 we show the overall bifurcation diagram for the three sequences of global bifurcations.

6.2. *Route to chaos starting from the supercritical Hopf bifurcation, sequence 1*

Supercritical Hopf bifurcation ($B1.1$ in figure 3) occurs at $\sigma = \sigma_{H1} = 0.292479$ and two stable limit cycles occur at fixed points A and B respectively. They are symmetric in the sense discussed above and will be referred to as periodic orbits A and B. The sizes of these orbits increase as σ is increased to $\sigma = 0.323076$.

At $\sigma = 0.323076$ one Floquet multiplier of each periodic orbit A and B leaves the unit circle at -1 and period-doubling bifurcations occur. A period-doubling sequence is then established ($B1.2.1$–$1.2.\infty$). If we denote the period at the point of the first period doubling as T, then in figure 4 we show projections on the (x_1, x_2) coordinate planes of the periodic motion of period $4T$, designated A^4 in figure 3, since it is in

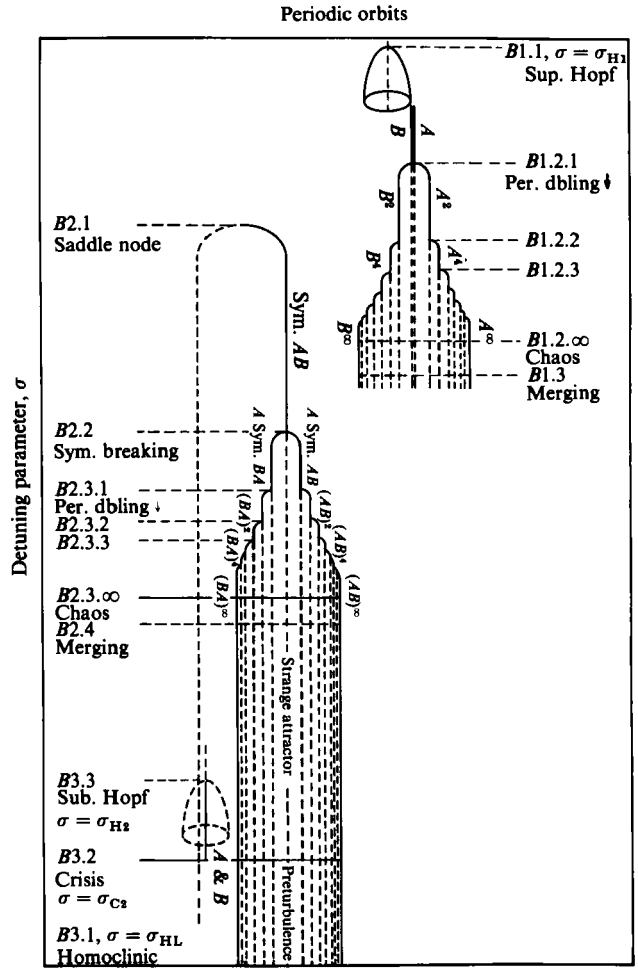

FIGURE 3. Global bifurcations to chaotic motions for $\beta = -1.0$ and $d = 0.1$. ——, stable orbits; – – – –, unstable orbits.

the part of the space dominated by A. By using the universal constant of Feigenbaum (1978), we predict that the period-doubling sequence terminates in chaotic motions at $\sigma = \sigma_F = 0.323765$. We present in figure 5(*a*) the projection of the chaotic motion, when $\sigma = 0.323800$, again around A, on the same coordinate planes. Also given in figure 5(*b*) is the power spectrum of the motion. A similar sequence of bifurcations occurs around the fixed point B.

With a small further increment of σ to the value $\sigma = 0.32400$, the separate chaotic motions around A and B merge in a global bifurcation ($B1.3$) as shown in figure 6.

Bifurcation sequences 2 and 3, discussed below, approach chaotic behaviour with σ increasing and decreasing respectively. It is suspected that these sequences are related to the occurrence of a homoclinic orbit at $\sigma = \sigma_{HL} = 0.4955316$.

6.3. *Route to chaos starting from a saddle-node bifurcation, sequence 2*

At $\sigma = 0.323640$ a saddle-node bifurcation ($B2.1$) of global periodic orbits occurs. Of the two orbits the stable one is shown in projections on (x_1, y_1)-coordinate plane in figure 7. We note that the orbit is large enough to encompass portions of the space

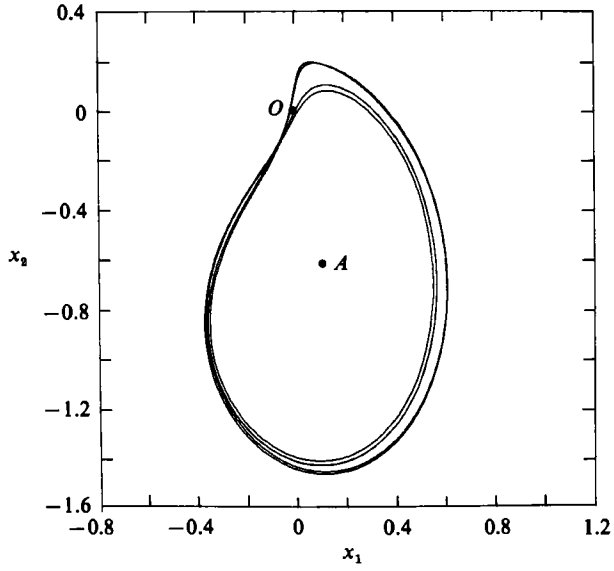

FIGURE 4. Stable periodic orbit A^4 at $\sigma = 0.323700$.

dominated by both fixed points A and B and for this reason it is indicated as AB in figure 3. We note, furthermore, that the value of $\sigma = 0.32364$ overlaps the values of σ for the bifurcation sequence 1, and thus, this bifurcation occurs simultaneously with the other bifurcations, that occur closer to A and B, labelled $A^2, A^4, \ldots, B^2, B^4, \ldots$, etc. The large stable periodic orbit AB grows in size with σ until $\sigma = 0.384000$, at which value a symmetry-breaking bifurcation ($B2.2$) occurs. This is a pitchfork bifurcation and occurs when one of the Floquet multipliers of the periodic orbit AB passes through $+1$. This bifurcation leads to two stable asymmetric periodic orbits labelled AB and BA respectively in figure 3. Each of these asymmetric periodic orbits now begins other period-doubling sequences $(AB)^2, (BA)^2, (AB)^4, \ldots$, with the Floquet multiplier going through -1 each time. They are labelled $B2.3.1.$ and $B2.3.2, \ldots$, in figure 3. Stable periodic orbits of period T, $2T$, $4T$ and $8T$ (not the T mentioned earlier) were observed at $\sigma = 0.385980$, 0.386001, 0.386200, 0.386230, respectively. In figure 8 we show the orbit $(BA)^4$. The computed value of the Feigenbaum ratios δ_j is quite close to the universal constant $\delta = 0.466920$ and the accumulation point for chaotic motion for one-sided chaos ($B2.3.\infty$) is estimated to be $\sigma = 0.386237$, by using $\sigma = 0.385995$ as the starting value and using the above universal constant. In figure 9 we show asymmetric chaotic behaviour of the solution at $\sigma = 0.386390$. We note that a similar chaotic motion coexists at this value of σ. A further increase in σ leads to another merging at $\sigma = 0.386395$ ($B2.4$) when the two asymmetric chaotic motions collide. We show this motion in figure 10.

We note that none of the equilibrium points O, A or B are stable when the above-mentioned chaotic motion occurs. In order to understand the nature of the phenomena better, we have taken a three-dimensional Poincaré section at y_1 very close to zero ($y_1 = 10^{-6}$). The resulting map is shown in figure 11. We note that $x_1 = y_1 = 0$ is an invariant set and there are no points on $x_1 = 0$. The map appears to be in two parts which tangent the $x_1 = y_1 = 0$ subspace. Each part, however, is not separately invariant, the solution freely going from one part to the other and thus there is a true merging of the two attractions.

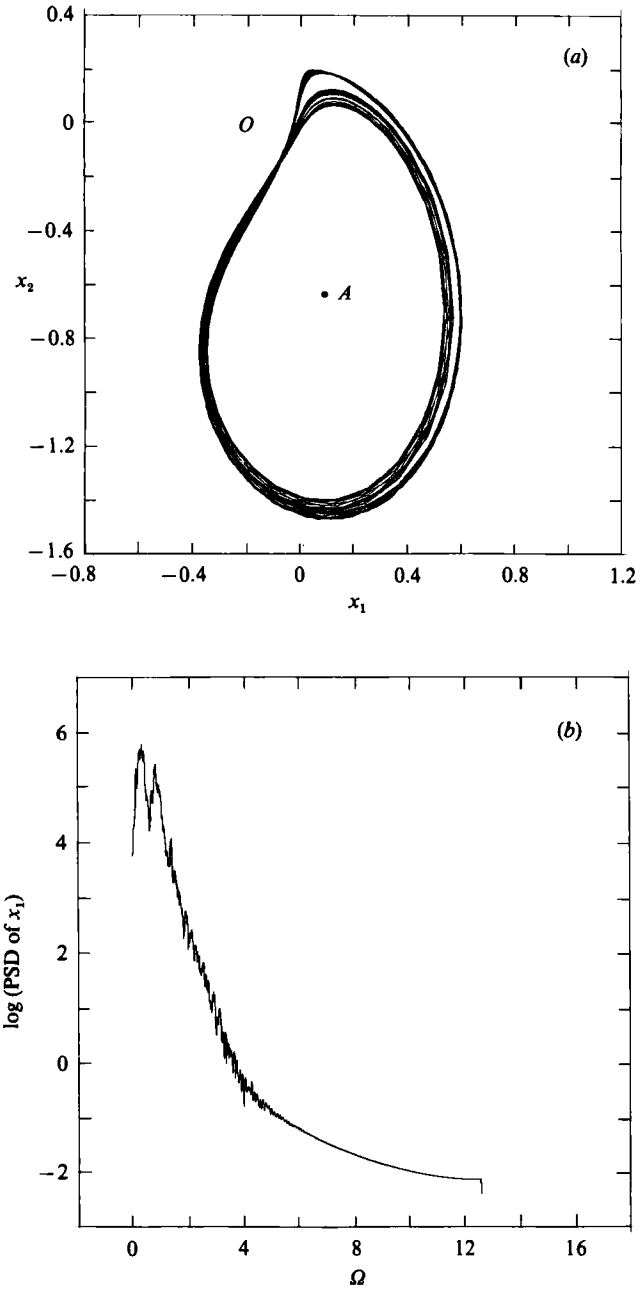

FIGURE 5. (*a*) One-sided chaotic motion at $\sigma = 0.323800$.
(*b*) Power spectrum of chaotic motion at $\sigma = 0.323800$.

6.4. *Route to chaos starting with a homoclinic orbit–Šilnikov phenomena, sequence 3*

There is strong evidence of a homoclinic orbit for $0.495\,531\,56 < \sigma < 0.495\,531\,64$. We recall that for σ taking these values the origin has a one-dimensional unstable manifold and a three-dimensional stable manifold, while both A and B are stable fixed points. Numerical integrations were done with initial conditions as close as possible

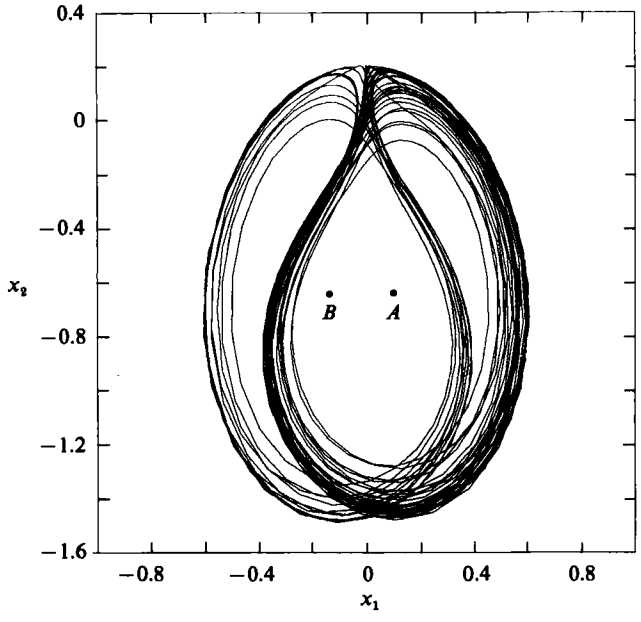

FIGURE 6. Chaotic motion at $\sigma = 0.324000$.

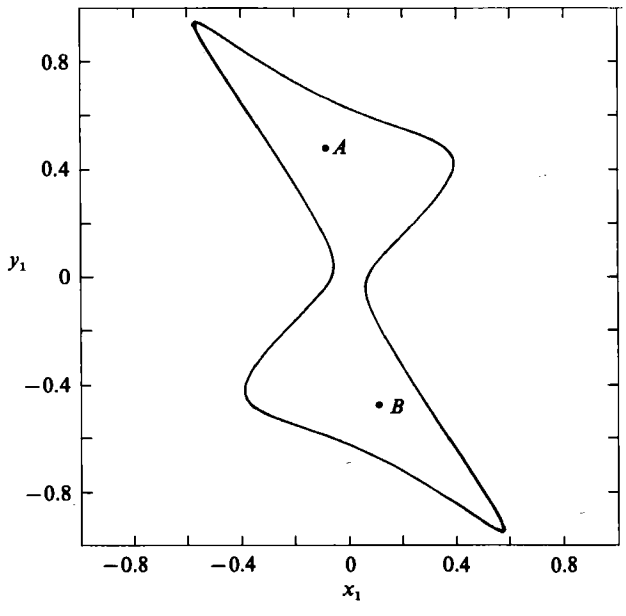

FIGURE 7. Stable symmetric periodic orbit AB at $\sigma = 0.323600$.

to the origin and on the eigenvector corresponding to the positive eigenvalue, i.e. on the unstable manifold. The solution gives an approximation to the one-dimensional global unstable manifold of the origin. When $\sigma = 0.495\,531\,64$ the orbit tends to stay in the 'same' subspace, say the one dominated by A, and tends to return to points very close to O (see figure 12a) before it goes to A for large t. If $\sigma = 0.495\,531\,56$, on

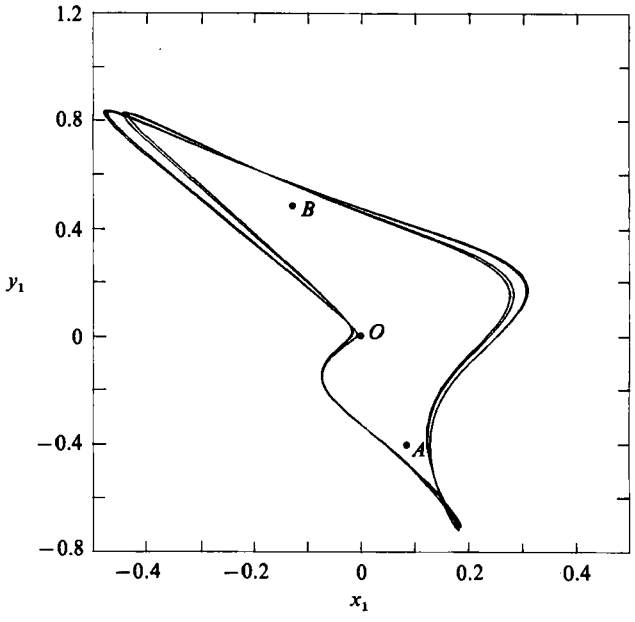

FIGURE 8. Stable asymmetric periodic $(BA)^4$ at $\sigma = 0.386200$.

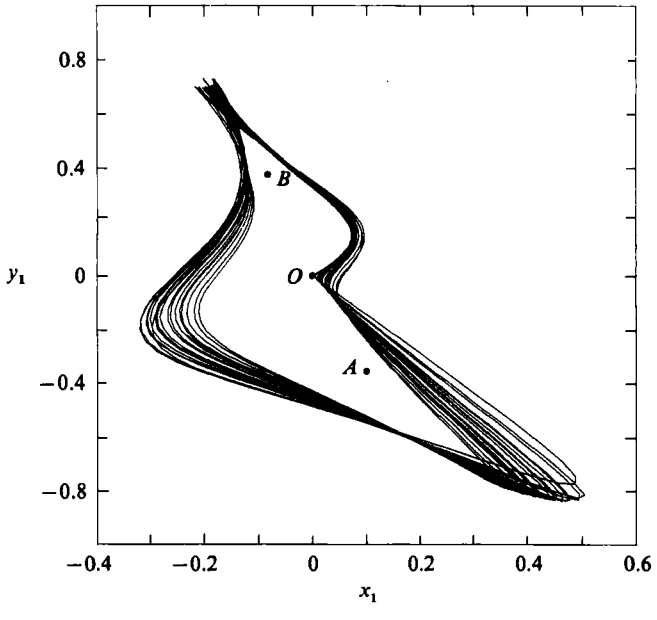

FIGURE 9. One-sided chaotic motion at $\sigma = 0.386390$.

the other hand, the trajectory with the same initial conditions again returns very close to the origin (see figure 12*b*) but then tends to the subspace dominated by B, and if observed for long enough time, would go to B as $t \to \infty$. Thus, for some critical value $\sigma = \sigma_{\mathrm{HL}}$ in between these values, we expect a homoclinic orbit and a homoclinic bifurcation ($B3.1$). Furthermore, there is additional evidence based on computer

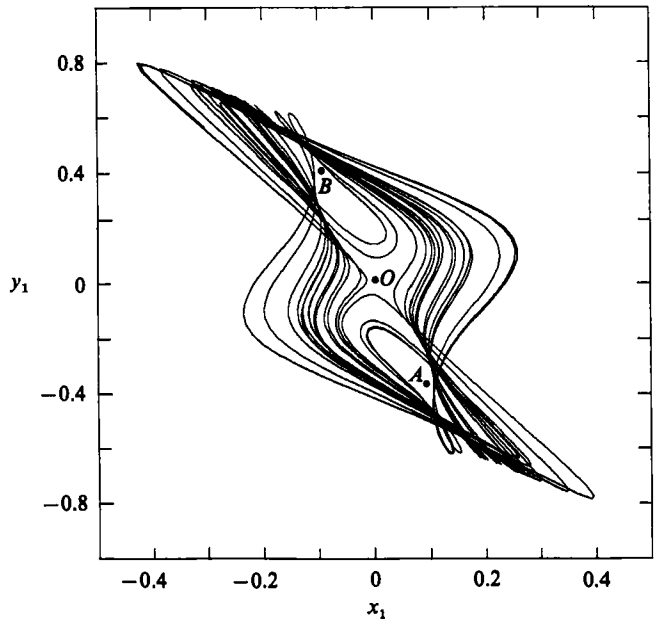

FIGURE 10. Chaotic motion at $\sigma = 0.4000000$.

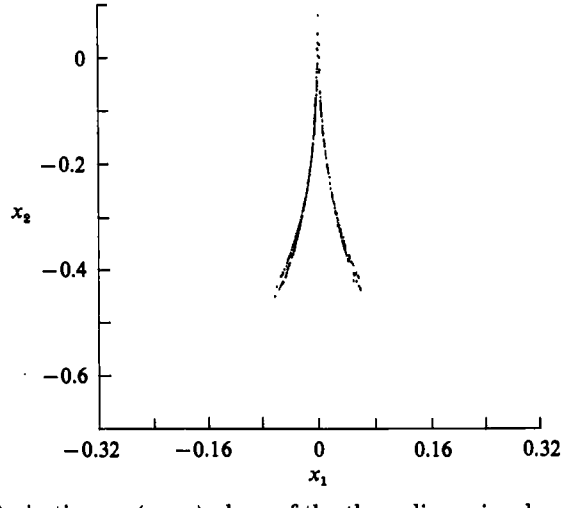

FIGURE 11. Projection on (x_1, x_2)-plane of the three-dimensional map at $\sigma = 0.386390$.

simulations that the unstable periodic orbits generated by the subharmonic Hopf bifurcations at $\sigma = \sigma_{H2}$ at both A and B, grow as σ is increased from $\sigma = \sigma_{H2}$ and eventually touch the origin and become the homoclinic orbit discussed above.

For values of σ $(\sigma_{C2}, \sigma_{HL})$ where $\sigma_{C2} \approx 0.4715$, orbits starting near the origin have chaotic transients before they eventually go to the fixed point in the subspace opposite to the direction of the initial conditions, the transients becoming very long when σ approaches σ_{C2} from above. This implies that Smale horseshoes have been created in the homoclinic bifurcation and preturbulence phenomena are occurring.

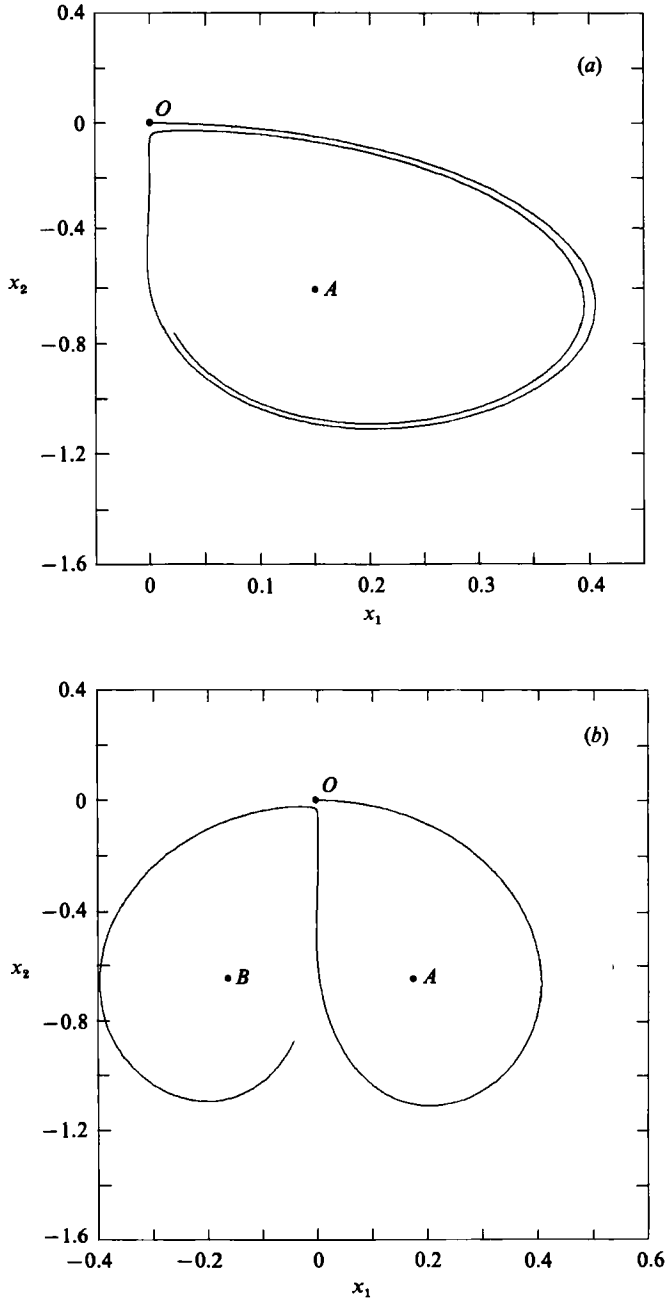

FIGURE 12. (*a*) Unstable manifold of the origin at $\sigma = 0.49553164$.
(*b*) Unstable manifold of the origin at $\sigma = 0.49553156$.

For $\sigma_{H2} < \sigma < \sigma_{C2}$, numerical integrations show that orbits starting near the origin no longer tend to A or B as $t \to \infty$, even though A and B are stable. To understand this behaviour, a study of the unstable periodic orbits at the subcritical Hopf bifurcations at A and B was made. Of the four Floquet multipliers for each periodic orbit, one multiplier is one, two multipliers have moduli less than one, and

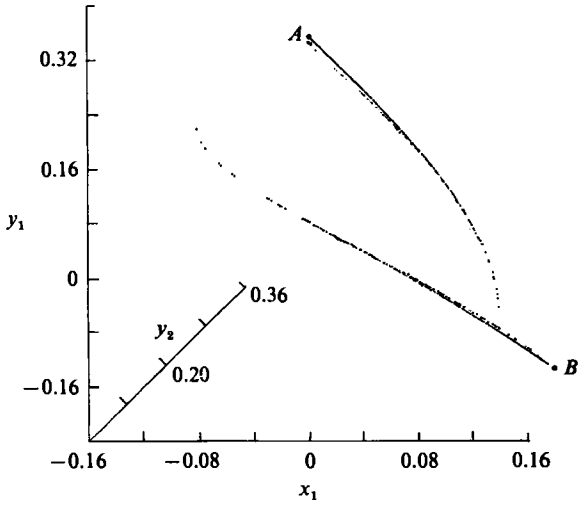

FIGURE 13. Three-dimensional map at $\sigma = 0.471000$.

one multiplier has modulus greater than one. Thus, each of the unstable periodic orbits, which are very close to A and B, has a three-dimensional stable manifold, which apparently effectively separate the basin of attraction of the fixed points from that of the strange invariant set and a strange attractor is formed.

To confirm the above conjecture, a three-dimensional map on a Poincaré section on the hyperplane, $x_2 = x_{2A} = x_{2B}$, where x_{2A} and x_{2B} are the x_2-coordinates of A and B respectively, was taken. The fixed points A and B, of course, appear as fixed points on this Poincaré section. For σ in the preturbulence range, $\sigma_{C2} = 0.4715 < \sigma < 0.4965$, A and B lie in the invariant set, and as σ approaches σ_{H2} from above, points A and B move to the edge of the strange invariant sets, and for $\sigma = \sigma_{C2}$ they leave the set, figure 13. Such a global change sometimes is called a crisis (Grebogi, Ott & Yorke 1983).

We note for σ slightly larger than the value of σ_{HL}, at which homoclinic phenomena occur, no chaotic phenomena are observed while the theorem of Šilnikov assures the existence of a horseshoe in an open interval around σ_{HL}. There are two explanations for this. One is due to the fact that the imaginary part of the complex eigenvalues takes a very small value when $\sigma = \sigma_{HL}$. Glendenning & Sparrow (1984) remark that when this happens the effects of the horseshoes are hard to detect with numerical techniques for parameter values on one side of the critical value of the parameter.

There is another explanation of the apparent asymmetry. A research effort has been initiated to study the four-dimensional Šilnikov phenomena in greater detail employing the procedures of Glendenning & Sparrow (1984). Preliminary investigation shows that, in the case of four dimensions, the value of the fourth real eigenvalue plays an important role. Under the Šilnikov restrictions on the eigenvalues, the additional real negative eigenvalue introduces an asymmetry in the following sense. If $\sigma = \sigma_{HL}$ is the value of σ at homoclinicity, then although the horseshoe is present for σ in an open interval containing σ_{HL}, i.e. $\sigma(-\epsilon_1 + \sigma_{HL}, \sigma_{HL} + \epsilon_2), \epsilon_1 > 0, \epsilon_2 > 0$, the value of $\epsilon_2 \ll \epsilon_1$, and thus computer calculations may not show chaotic phenomena for $\sigma > \sigma_{HL}$.

7. Difficulties of experimental confirmation

Efforts were made with equipment similar to that used by Virnig, Berman & Sethna (1987) to check the chaotic phenomena predicted by the theory. The efforts were unsuccessful, primarily due to the effect of energy dissipation. In order to satisfy all the requirements of space and dynamic coupling for a fluid with relatively small surface tension, the fluid depth required is quite small and for shallow water waves the dissipation of energy due to boundary effects appears to discourage the phenomena.

An alternate formulation of the problem would, we think, lead to experimental verification of the theory, but this has not been done due to lack of appropriate equipment. A careful examination of the equations shows that equations of identical structure, but with different values of dimensionless parameters, are obtained when one studies the motion of the interface layer between two immiscible fluids of different densities enclosed in a rectangular box. If the densities of the fluids are not very different, the surface-tension effects on the interface become dominant compared to the gravity effect and it is possible to have wave motions of the type discussed here with both fluids having fairly large depths. The difficulty of the experiment arises from the fact that the container needs to be given a fairly large vertical motion to excite the waves, because it is the difference in the densities that generate the phenomenon. In Gu *et al.* (1987) and Virnig *et al.* (1987), a theory based on one-mode analysis has been verified experimentally. Since the analysis here is based on assumptions that are very similar to those in these references, it should be possible to verify experimentally the theory for waves at the interface of two fluids.

8. Remark

We have described a system that, at least in theory, will show chaotic behaviour for two of its spatial modes. The question arises as to whether the analysis can be generalized so that the surface waves would appear to have more complex behaviour. It appears that the several requirements that lead to chaotic behaviour are likely to be satisfied more easily in a more elaborate analysis involving several modes doing large motions. A study of the diaphantine equations (3.8) for several modes shows that many combinations of modes will satisfy these equations. Furthermore, the additional requirements of resonant coupling between modal frequencies would impose conditions on sum and difference of several modal frequencies and would, in general, be more easily satisfied without forcing the requirement of shallow fluid depth. The Šilnikov theory itself is valid in higher dimensions and, in general, the higher dimensional problems will have more parameters, and there would be a greater probability of finding a combination of these parameters that will satisfy the dual requirements of homoclinicity and conditions on the eigenvalues. In view of all this, it appears likely that a more elaborate analysis would show more complex phenomena.

This work was supported by Grant NSF-MEA 8310966. The authors wish to acknowledge the help of Mr John Vernig in connection with some experiments related to this work.

Appendix. Definitions and calculations of coupling coefficients

It can be shown that the eigenfunctions evaluated at the free surface are a complete set:

$$S_{ij} = \cos\frac{i\pi x}{a}\cos j\pi y \quad (i,j = 0,1,2,\ldots), \tag{A 1}$$

The inner product of any two elements of (A 2) is defined as

$$\langle S_{ij}, S_{rs}\rangle \overset{\text{def}}{=} \frac{4}{a}2^{-(\delta_{0r}+\delta_{0s})}\int_0^a\int_0^1 S_{ij}S_{rs}\,\mathrm{d}x\,\mathrm{d}y, \tag{A 2}$$

where δ_{0r} and δ_{0s} are the Kronecker deltas, and a direct result from (A 2) is

$$\langle S_{ij}, S_{rs}\rangle = \delta_{ir}\delta_{js}, \tag{A 3}$$

where δ_{ir} and δ_{js} are the Kronecker deltas.

Listed below are the definitions of the coupling coefficients:

$$G^{(1)\,mn}_{ijrs} = \left\langle\frac{\partial S_{ij}}{\partial x}\frac{\partial S_{rs}}{\partial x}, S_{mn}\right\rangle + \left\langle\frac{\partial S_{ij}}{\partial y}\frac{\partial S_{rs}}{\partial y}, S_{mn}\right\rangle - K_{rs}^2\langle S_{ij}S_{rs}, S_{mn}\rangle,$$

$$G^{(2)\,mn}_{ijrs} = \left\langle\frac{\partial S_{ij}}{\partial x}\frac{\partial S_{rs}}{\partial x}, S_{mn}\right\rangle + \left\langle\frac{\partial S_{ij}}{\partial y}\frac{\partial S_{rs}}{\partial y}, S_{mn}\right\rangle + \alpha_{ij}\alpha_{rs}\langle S_{ij}S_{rs}, S_{mn}\rangle,$$

$$G^{(3)\,mn}_{ijrs} = \alpha_{rs}\langle S_{ij}S_{rs}, S_{mn}\rangle.$$

In the special cases when (i,j) is either $(2m,2n)$, $(2m,0)$, $(0,2n)$ or $(0,0)$ the coupling coefficients take the special forms:

$$G^{(1)\,ij}_{mnmn} = -\tfrac{1}{2}(n\pi)^2\delta_{0i}\delta_{2nj} - \frac{1}{2}\left[\frac{m\pi}{\lambda_1}\right]^2\delta_{2mi}\delta_{0j} - \tfrac{1}{2}K_{mn}^2\delta_{2mi}\delta_{2nj},$$

$$G^{(2)\,ij}_{mnmn} = \frac{1}{4}\left[\left(\frac{m\pi}{a}\right)^2 - (n\pi)^2 + \alpha_{mn}^2\right]\delta_{0i}\delta_{2nj} + \frac{1}{4}\left[-\left[\frac{m\pi}{a}\right]^2 + (n\pi)^2 + \alpha_{mn}^2\right]\delta_{2mi}\delta_{0j}$$
$$+\tfrac{1}{4}(-K_{mn}^2 + \alpha_{mn}^2)\,\delta_{2mi}\delta_{2nj},$$

$$G^{(3)\,ij}_{mnmn} = \tfrac{1}{4}\alpha_{mn}2^{\delta_{m0}+\delta_{n0}},$$

$$G^{(1)\,mn}_{ijmn} = \frac{1}{4}\left[\left(\frac{im}{a^2}+jn\right)\pi^2 - K_{mn}^2\right]2^{\delta_{0i}+\delta_{0j}},$$

$$G^{(1)\,mn}_{mnij} = \frac{1}{4}\left[im\left(\frac{\pi}{a}\right)^2 + jn\pi^2 - K_{ij}^2\right]2^{\delta_{0i}+\delta_{0j}},$$

$$G^{(2)\,mn}_{ijmn} = \frac{1}{4}\left[\left(\frac{im}{a^2}+jn\right)\pi^2 + \alpha_{ij}\alpha_{mn}\right]2^{\delta_{0i}+\delta_{0j}},$$

$$G^{(2)\,mn}_{mnij} = G^{(2)\,mn}_{ijmn},$$

$$G^{(3)\,mn}_{ijmn} = \tfrac{1}{4}\alpha_{mn}2^{\delta_{0i}+\delta_{0j}},$$

$$G^{(3)\,mn}_{mnij} = \tfrac{1}{4}\alpha_{ij}2^{\delta_{0i}+\delta_{0j}}.$$

In the above expressions, α_{ij} is defined by

$$\alpha_{ij} = K_{ij}\tanh K_{ij}a.$$

In case of $(i,j) = (2m, 2n)$, the expressions of Γ_{mn} and Γ_{ij} in (4.4) and (4.5) can be reduced to

$$\Gamma_{mn} = \tfrac{1}{32} K_{mn}(3 - \tanh^2 K_{mn} h)/\tanh K_{mn} h \cdot 2^{\delta_{0m}+\delta_{0n}},$$

$$\Gamma_{ij} = \frac{\Gamma_{mn}}{1 + \tanh^2 K_{mn} h}.$$

REFERENCES

Bajaj, A. K. & Sethna, P. R. 1980 Hopf bifurcation phenomena in tubes carrying a fluid. *SIAM J. Appl. Maths* **39**, 213–230.

Benjamin, T. B. & Ursell, F. 1954 The stability of the plane free surface of a liquid in vertical periodic motion. *Proc. R. Soc. Lond.* A **225**, 505–517.

Ciliberto, S. & Gollub, J. P. 1984 Pattern competition leads to chaos. *Phys. Rev. Lett.* **52**, 922–925.

Ciliberto, S. & Gollub, J. P. 1985 Chaotic mode competition in parametrically forced surface waves. *J. Fluid Mech.* **158**, 381–398.

Faraday, M. 1831 On the forms and states assumed by fluids in contact with vibrating elastic surfaces. *Phil. Trans. R. Soc. Lond.* **121**, 39–346.

Feigenbaum, M. J. 1978 Quantitative universality for a class of non-linear transformations. *J. Stat. Phys.* **19**, 25–52.

Gavrilov, N. K. & Šilnikov, L. P. 1972 On three-dimensional dynamical systems close to systems with a structurally unstable homoclinic curve. I. *Math. USSR Sbornik* **17**, 467–485.

Gavrilov, N. K. & Šilnikov, L. P. 1973 On three-dimensional dynamical systems close to systems with a structurally unstable homoclinic curve. II. *Math. USSR Sbornik* **19**, 139–156.

Glendenning, P. & Sparrow, C. 1984 Local and global behavior near homoclinic orbits. *J. Stat. Phys.* **35**, 645–696.

Grebogi, C., Ott, E. & Yorke, J. A. 1983 Crisis, sudden changes in chaotic attractors and transient chaos. *Physica* **7D**, 181–200.

Gu, X. M. 1986 Nonlinear surface waves of a fluid in rectangular containers subjected to vertical periodic excitations. Ph.D. thesis, University of Minnesota.

Gu, X. M., Sethna, P. R. & Narain, A. 1987 On three-dimensional non-linear subharmonic resonant surface waves in a fluid. Part I: Theory. *Trans. ASME* E: *J. Appl. Mech.* (submitted).

Guckenheimer, J. & Holmes, P. 1983 *Nonlinear Oscillations, Dynamical Systems and Bifurcation of Vector Fields*. Springer.

Hale, J. K. 1969 *Ordinary Differential Equations*. Wiley-Interscience.

Holmes, P. J. 1986 Chaotic motions in a weakly nonlinear model for surface waves. *J. Fluid Mech.* **162**, 365–388.

Kaplan, J. L. & Yorke, J. A. 1979 Preturbulence, a regime observed in a fluid flow model of Lorenz. *Commun. Math. Phys.* **67**, 93–108.

Lichtenberg, A. J. & Lieberman, M. A. 1982 *Regular and Stochastic Motion*. Springer.

Lorenz, E. N. 1963 Deterministic non-periodic flows. *J. Atmos. Sci.* **20**, 130–141.

Lorenz, E. N. 1984 The local structure of a chaotic attractor in four dimensions. *Physica* **13D**, 90–104.

Meron, E. & Procaccia, I. 1986 Theory of chaos in surface waves equals the reduction from hydrodynamics to few-dimensional dynamics. *Phys. Rev. Lett.* **56**, 1323–1326.

Miles, J. W. 1967 Surface-wave damping in closed basins. *Proc. R. Soc. Lond.* A **297**, 459–475.

Miles, J. W. 1976 Nonlinear surface waves in closed basins. *J. Fluid Mech.* **75**, 419–448.

Miles, J. W. 1984*a* Nonlinear Faraday resonance. *J. Fluid Mech.* **146**, 285–302.

Miles, J. W. 1984*b* Internally resonant surface waves in a circular cylinder. *J. Fluid Mech.* **149**, 1–14.

Miles, J. W. 1984*c* Resonantly forced surface waves in a circular cylinder. *J. Fluid Mech.* **149**, 15–31.

MILES, J. W. 1985 Resonantly forced, non-linear gravity waves in a shallow rectangular tank. *Wave Motion* **3**, 291–297.

MITROPOLSKY, Y. A. 1965 *Problems of Asymptotic Theory of Non-Stationary Vibrations.* Israel Program for Scientific Translations, Jerusalem.

ROUTH, E. J. 1877 *Dynamics of a System of Rigid Bodies.* Macmillan.

SETHNA, P. R. & GU, X. M. 1985 On global motions of articulated tubes carrying a fluid. *Intl J. Non-Linear Mech.* **20**, 453–469.

ŠILNIKOV, L. P. 1970 A contribution to the problem of the structure of an extended neighborhood of a rough equilibrium state of saddle-focus type. *Math. USSR Sbornik* **10**, 91–102.

VIRNIG, J. C., BERMAN, A. S. & SETHNA, P. R. 1987 On the three-dimensional nonlinear subharmonic resonant surface waves in a fluid. Part II: Experiment. *Trans. ASME* E: *J. Appl. Mech.* (submitted).

YORKE, J. A. & ALLIGOOD, K. T. 1985 Period doubling Cascades of attractors: A prerequisite for horseshoes. *Commun. Math. Phys.* **101**, 305–321.